



## FABRICATION OF PdNPs DECORATED TiO<sub>2</sub> NANOTUBES BY ELECTRODEPOSITION METHOD AS ANTICANCER MATERIALS

Shaymaa R. Baqer\*, Mahasin Alias and Abdulkareem M. Ali Alsammarraie

Department of Chemistry, College of Science for Women, University of Baghdad, Baghdad, Iraq

\*Corresponding author email : shyma0213@gmail.com

### Abstract

In this study palladium nanoparticles were prepared from using five derivatives of Mannich base palladium complexes which have been used as sources of palladium and decorated on TiO<sub>2</sub>NTs by using electrodeposition method. Prepared and investigated the physical properties of the anatase TiO<sub>2</sub>NTs phase before and after deposition Pd nanoparticles by using X-ray diffraction spectroscopy, transmission electron microscopy (TEM), field emission scanning electron microscope (FE-SEM), energy dispersive X-ray (EDX), and FT-IR technique and comprehensively investigated the effect of cytotoxic depending on the crystal form of TiO<sub>2</sub>NTs and Pd/TiO<sub>2</sub>NTs by using two type of cell lines cancer (MCF-7) and normal (WRL68). The result show that the inhibitory of cancer cell line increases when the palladium nanoparticles are deposited on the TiO<sub>2</sub>NTs surfaces.

**Keywords:** Electrodeposition, Pd nanoparticles, Titanium dioxide nanotube, Cytotoxic assay, Anticancer evolution.

### Introduction

Nanoparticles have received much attention in present scenario due to their application in cancer therapy. Based on clinical efficacy, TiO<sub>2</sub>NTs has a very wealthy data related to cytotoxicity. The cheapest and most easy method that leads to ordered TiO<sub>2</sub> nanotube array is anodization technique Escada *et al.* (2017). There are many factors that affects in anodizing process such as anodization time Indira *et al.* (2015), temperature Ayal *et al.* (2016). anodization potential Indira *et al.* (2015), and Ayal *et al.* (2016), and the electrolyte Indira *et al.* (2015) and Ayal *et al.* (2016), thus its effect on the diameter, thickness and pores of nanotubes by controlling the anodization conditions, many types of TiO<sub>2</sub> nanotubes such as ripples free or double-wall can be formed Robin *et al.* (2014). In the past, palladium as a member of the platinum group metals was mainly known as an expensive noble metal. Palladium belongs to group ten in the periodic table Saldan *et al.* (2015). Palladium NPs have invaluable mechanical, optical and catalytic, properties that are in widely used in industrial applications as well as anticancer and antibacterial activity Leso and IavicoliInt (2018), Siddiqi, and Husen (2016), and Veena (2018).

Doping of TiO<sub>2</sub>NPs with noble metals such as silver, gold or platinum reduces the energy gap and hence the light response in the visible area N., Feng, *et al.* (2013). Generating ROS and their potential applications by doped TiO<sub>2</sub>NPs which make them active under visible light have been recently investigated in death of microbial group Jiang *et al.* (2015), and Boxi *et al.* (2016). Thus, some studies have shown that doped TiO<sub>2</sub> can death bacteria without any light illumination and can be activated under normal light Paul *et al.* (2016) and Lin *et al.* (2011).

In the following paper Pd nanoparticles has been used to modify the surface of titania nanotubes and used as an anticancer material from different of Mannich bases palladium complexes at fixed concentration and time. The ligands act as organic material that prevent the accumulation of palladium nanoparticles during the electro deposition. In vitro two types of cancer (breast cancer) and normal cell lines were used.

### Material and Methods

All chemicals were purchased from commercial sources H<sub>2</sub>PtCl<sub>6</sub>·6H<sub>2</sub>O (99.9%), S-(1-(benzothiazole-2-ylamino) methyl]-H-benzimidazole-2-yl) 4-nitrobenzothioate (L<sub>1</sub>), S-(1-(Pyrazine-2-carboxamido) methyl) -1-H-benzoimidazole-2-yl) 4-nitrobenzo thiolate (L<sub>2</sub>), N-((2-((Morpholinomethyl) thiol)-1H-benzimidazol-yl) methyl) pyrazine-2-carboxamide (L<sub>3</sub>), 2-(Morpholin-N-methyl)mercapto-1H-benzimidazole (L<sub>4</sub>), S-(1-Morpholinomethyl)-1-benzimidazol-2-yl) 4-nitrobenzothio ate (L<sub>5</sub>) as the ligands. NH<sub>4</sub>F (99.5%), ethylene glycol 99.8% and Ti, Pt foil (99.6, 99.99% ) with thickness 0.25 mm. Solvents and reagents were used as received. The nanostructures were characterized by FE-SEM, TEM, XRD, EDX and FT-IR. Transmission Electron microscopy (TEM) was recorded on Philips CM (10). Atomic weight and atomic number of all prepared nanoparticles were carried out by energy dispersive X-ray spectroscopy (EDS) XFlah6-10 Detector –Bruker. X-ray diffraction was measured using Shimadzu ray 6000. The field emission scanning electron microscope measurements were obtained using Hitachi FE-SEM model S-4160, Japan, 0.5 - 20 KV and the FT-IR spectra were recorded using IR Prestige-21, Single Beam Path Laser, Shimadzu (8400).

### Preparation of TiO<sub>2</sub>NTs and Pd/TiO<sub>2</sub>NTs photoelectrodes

TiO<sub>2</sub>NT electrodes were produced by anodization according to procedure. For this, titanium sheets (99.9%, Sigma Aldrich) were previously cut (1.0cm × 2cm), degreased by sonication in detergent, deionized (DI) water, ethanol and acetone respectively for 10 min. and dried in an oven at 100 °C for 15 minutes. The TiO<sub>2</sub>NTs electrodes were prepared by anodization using two-electrode cell configuration, with Ti foils as anode and Pt foil as a cathode. The anodizing solution containing 0.5 wt.% NH<sub>4</sub>F, (99.5%) in anhydrous ethylene glycol (99.8%) and 5.0 Vol.% H<sub>2</sub>O at room temperature. The anodized substrate was then soaked in a water bath at 40 °C for 20 minutes to remove the organic electrolyte. The anodization was performed for one hours at 40 V. After the occurrence of the anode then, electrodes were fired at 550 °C during 2hrs in a muffle furnace to transform amorphous TiO<sub>2</sub> into crystalline anatase phase.

The Pd/TiO<sub>2</sub>NTs photoelectrodes were prepared by Pd nanoparticle deposition on TiO<sub>2</sub>NTs surface by using a conventional two-electrode electrochemical cell with graphite rod and TiO<sub>2</sub>NTs template was used for deposition. The electrolyte solution was prepared by dissolving the 2mM from five complexes PdL<sub>1</sub>, PdL<sub>2</sub>, PdL<sub>3</sub>, PdL<sub>4</sub> and PdL<sub>5</sub> in 100 ml mixture solvent (dimethyl formamide, ethanol, deionized water (1:1:1)). Electrodeposition time was set at 3 min., while the PdL<sub>4</sub> at 6min. The electrodeposition voltage was fixed at 7 V and pH=5.5. The prepared Pd/TiO<sub>2</sub>NTs was washed several times with deionized water to remove the residue of the solutions and then dried in air.

### Preparation of complexes

These compounds were prepared according to Alias *et al.* (2017) and (2018).

### Cytotoxic assays

Cytotoxicity effect of TiO<sub>2</sub>NTs and PdNPs when deposition on TiO<sub>2</sub>NTs on MCF-7 and WRL68 cancer cell line, and normal cell lines were done in a sterile area using the biosafety conditions of the airflow cabinet. MCF-7, WRL68 cell lines used in this study were equipped from Biotechnology Center/Al-Nahrain University. The cells were cultured in (MEM) modified eagle's medium with serum ((100 U/ml) of antibiotic, ((100 µg)) of streptomycin/ml in incubator with (5% CO<sub>2</sub> at 37 °C). The survival or death of cells were determined using (3-(4,5-

dimethylthiazole-2-yl)-2,5-diphenyl Tetrazolium bromide ((MTT)) which is diagnosed by using spectro photometer. Plated with 96-well have been sterilized. After twenty-four hours, cells were treated with different concentrations of prepared compounds starting from the lowest concentration and incubated in (5% CO<sub>2</sub>) atmosphere with high humidity. After forty-eight hours of compounds exposure, the cells were incubated with (0.5 mg/ml, MTT) distilled water for another four hours at thirty-seven degrees. 10% of salt (sodium dodecyl sulphate) then incubated for two hours. Absorption was measured at the wave length 620 nm on a multi-well ELISA plate reader Freshney (2015).

### Results and Discussions

The field emission scanning electron microscope (FE-SEM) analysis was used to examine the surfaces and cross section morphology of TNTs template and doped TiO<sub>2</sub> with Pd nanoparticles. In FE-SEM image it is obvious that the formation of a self-organized and uniform nanotube layers with different tube diameters are possible to be achieved. Palladium nanoparticles were distributed uniformly on the surface and some were deposited into the nanotubes using electrochemical deposition method, with diameters in the range from 21 to 32 nm, where palladium nanoparticles gathered on the TiO<sub>2</sub> nanotubes. The palladium nanoparticles have a distorted spherical shape, some of properties and particle size can be noticed in Table (1).

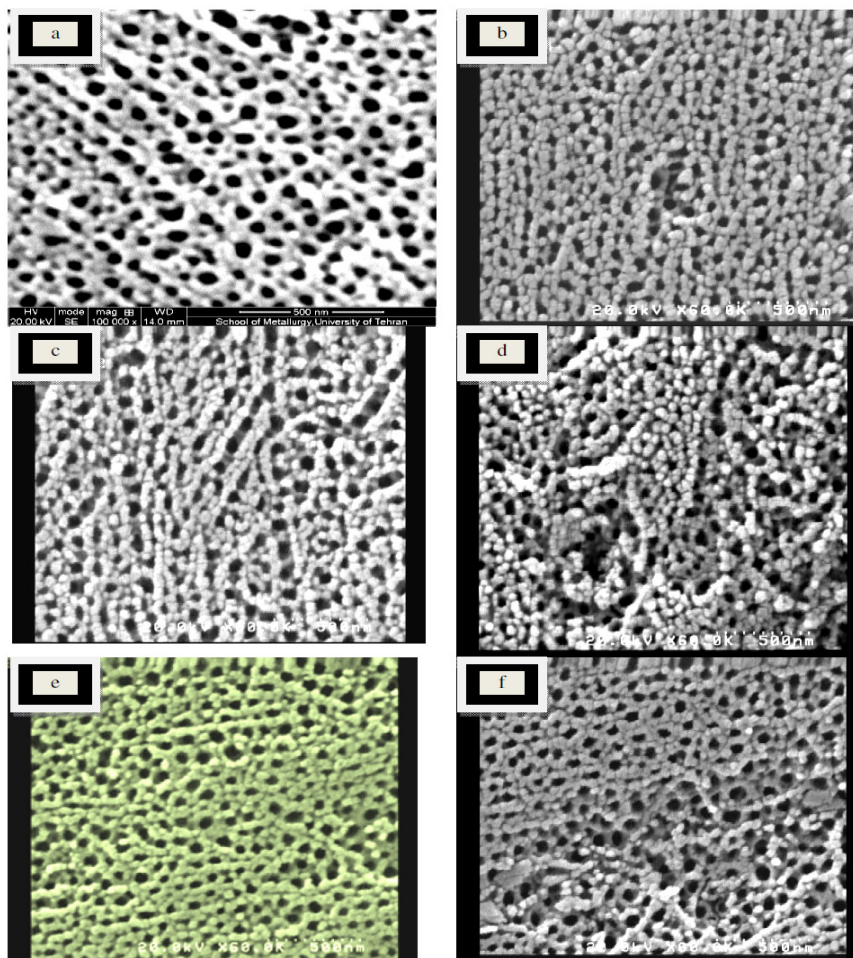


**Fig. 1 :** FE-SEM images (a)TNTs; (b,c,d,e,f) PdNPs decorated on TiO<sub>2</sub> NTs for all compounds

**Table 1 :** The range of particle size, outer and inner diameter of PdNPs/TiO<sub>2</sub>NTs

Sample	Diameter nm	Inner diameter	Particle size\nm
TiO <sub>2</sub> nanotube template	83	68	-----
PdL <sub>1</sub> NPs \TiO <sub>2</sub> NTs	89	49	21-30
PdL <sub>2</sub> NPs\ TiO <sub>2</sub> NTs	90	48	21-31
PdL <sub>3</sub> NPs\ TiO <sub>2</sub> NTs	93	43	24-32
PdL <sub>4</sub> NPs \TiO <sub>2</sub> NTs	90	46	22-31
PdL <sub>5</sub> NPs\ TiO <sub>2</sub> NTs	91	46	23-30

The following forms show the cross section of TiO<sub>2</sub>NTs and heavy metal Pd nanoparticles decorated on it, where the cross section shows the average length of the tubes is about 4 μm as shown in Figures (2). The cross-section shows that the

nanotubes are homogeneous and well-covered with small spaces between them, providing a suitable surface for deposition and a large area for penetrating the electrolyte solution.

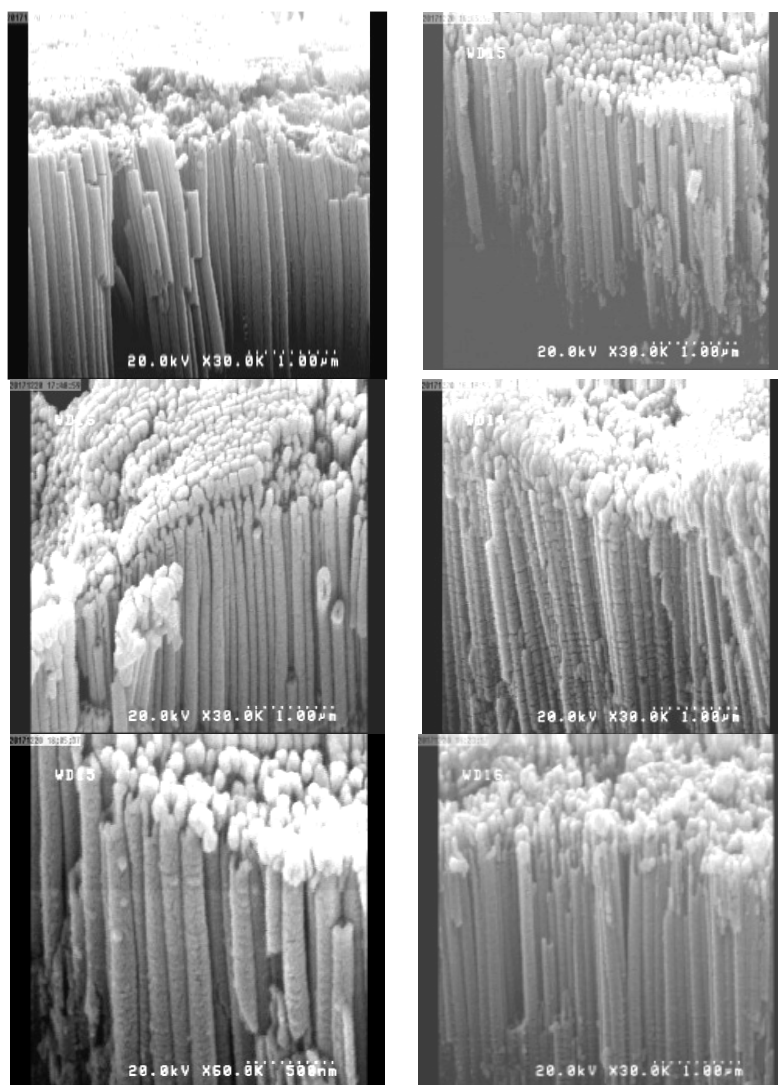


**Fig. 2:** Cross section images of (a) TNTs; (b) PdNPs deposited into TiO<sub>2</sub> NTs for all compounds

Figure 3 (a) & (b)) shows the TEM morphologies of titanium nanotubes before and after Pd deposition. TiO<sub>2</sub>NTs consist of a smooth wall with the average diameters of about 83 nm, which is in agreement with FE-SEM results, after palladium decorated, it can be seen that many Pd nanoparticles have been successfully decorated on the

internal and external walls of titanium nanotubes which is in agreement with the cross section FE-SEM results. TEM images of the TNTs and Pd and are represented in Figures (3 (a) & (b)). This result is coinciding with FE-SEM surface results.

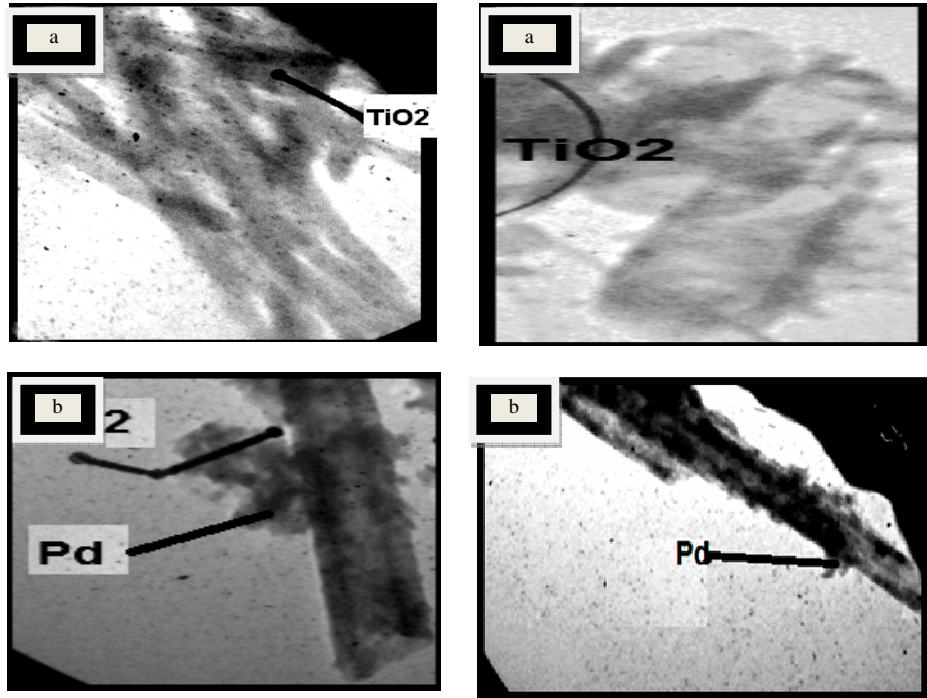


**Fig. 3 :** TEM images of (a) TiO<sub>2</sub>NTs; (b) Pd deposited into TiO<sub>2</sub> NTs

In EDX spectrum, the result is appeared in Figures (4). From the spectrum the presence of four peaks at 4.56, 0.423, 0.421 and 0.325 keV, sequentially are detect. The intense peaks are assigned to the Ti and the less intense refer to

oxygen and palladium deposition on it. This result confirms the existence of Pd atoms in the TiO<sub>2</sub> nanotubes. These values were ascertained after comparing them with references [18].

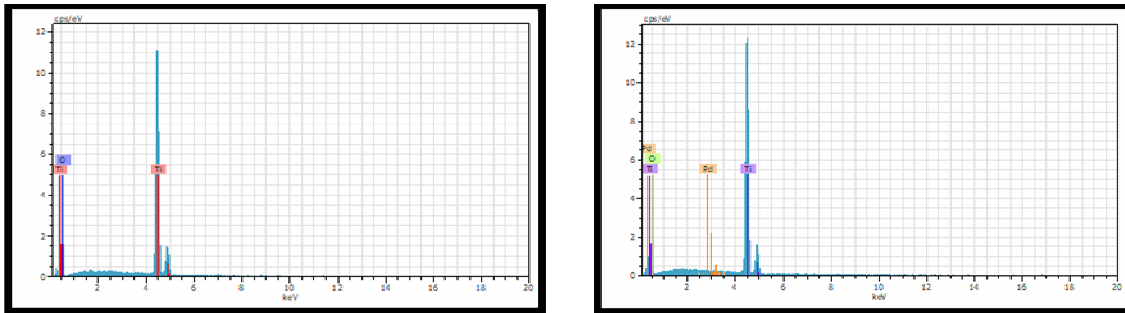


**Fig. 4 :** EDX analysis of TiO<sub>2</sub>NTs and PdNPs/TiO<sub>2</sub> nanotubes at 2mM

Raman measurements will prove to be invaluable for evaluating the crystalline phase uniformity of TiO<sub>2</sub>NTs .Titanium dioxide nanotubes have distortion octahedral shape in the anatase phase. The primitive unit cell has two TiO<sub>2</sub> units with Ti atoms ((0, 0, 0)) and ((0, 1/2, 1/4)) and O atoms ((0, 0, u)), ((0, 0,  $\bar{u}$ )), ((0, 1/2, u+1/4)) and ((0, 1/2, 1/2-u)) giving six active Raman modes: A<sub>1g</sub>+2B<sub>1g</sub>+3E<sub>g</sub>. Anatase phase of TiO<sub>2</sub> has vibrational modes at of Raman transitions and symmetry at 144, 197, 397, 517, 513, 639 cm<sup>-1</sup>, Figure (5) without any band for other phase (rutile or brookite) [19,20].

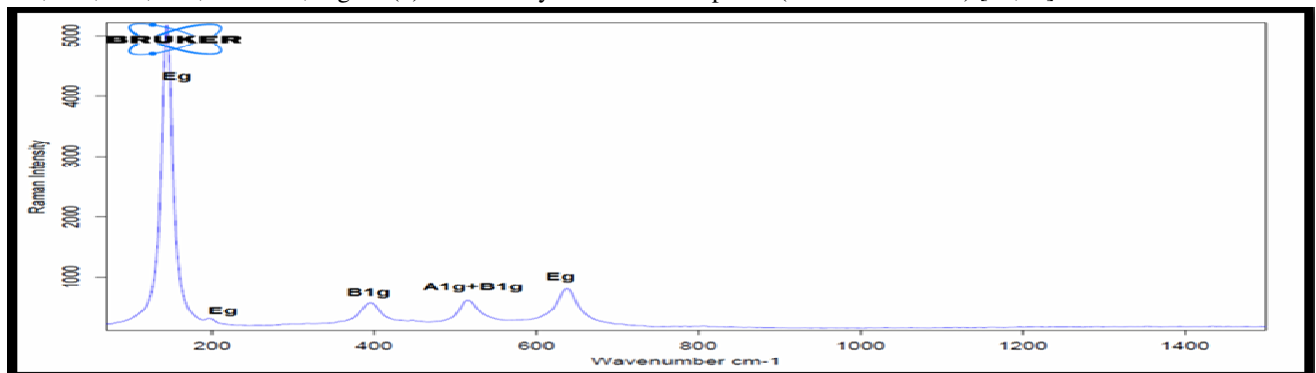


**Fig. 5:** Raman Spectrum of TiO<sub>2</sub>NTs

The structure and phase of the titanium dioxide nanotubes and the metallic salts deposited on it were recorded by X-ray diffraction (XRD) analysis. The XRD pattern exhibited the presence of titanium (JCPDS No. 44-1294), anatase (JCPDS No. 21-1272), diffraction peaks of TiO<sub>2</sub>  $2\theta = (25.44), (38.20), (48.29), (54.22), (55.30), (62.82), (70.48)$  and  $(75.58)^\circ$  Which belong to the (101), (004), (200), (105), (211), (204), (220) and (215) sequentially[14].

Crystallite size of TiO<sub>2</sub> was calculated from Scherer's equation which is equal to 59.6 nm. When deposition of Pd metals does not change in the form of the peaks of the anatase phase which may be attributed to low concentration of palladium in the solution of the complexes. These results correspond to the number of researches [21]. A comparison of XRD patterns /Pd samples was shown in Figures (6).

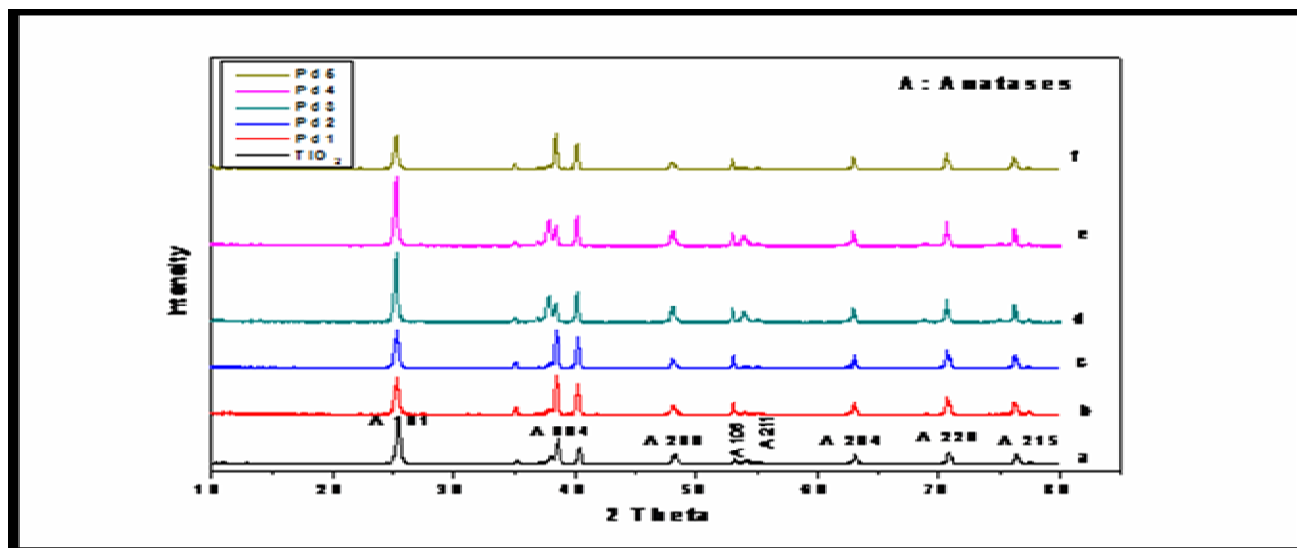


Fig. 6 : X-ray diffraction graphs of TiO<sub>2</sub>NTs and Pd nanoparticles when decorated on it (b,c,d,e,f)

From the result of the FT-IR spectrum of titanium dioxide nanotubes showed a broad band in the position 553-435 cm<sup>-1</sup> which due to the bending bands ( $\delta$ ) of (titanium-oxygen-titanium) [20]. The broad band observed around 3477-3338, and 1647, 1620 cm<sup>-1</sup>, this confirms the existence  $\nu(\text{OH})$  and  $\delta(\text{OH})$  group present in water molecules [22], which indicate absorption of some of the water molecules on the surface of TiO<sub>2</sub>NTs. All Pd nanoparticles in five complexes were showed approximately in the same position of TiO<sub>2</sub> nanotubes, this indicated no precipitate any organic compounds (Mannich bases) on the template of TiO<sub>2</sub>NTs.

#### Interpretation of cytotoxic assay results

The results were done on MCF-7, cell lines shown in Table (2) recorded the cytotoxicity effect of titana and Pd/TiO<sub>2</sub>NTs for 48 hrs exposure time .There was a significant difference ( $P < 0.05$ ), ( $t\text{-test} = 0.00$ ) at all

concentrations and compared to normal cell line at concentration (800, 400, 200, 100, 50, 25 and 12.5  $\mu\text{g/ml}$ ). Table (2) show the statistical results, and the value of IC<sub>50</sub> for MCF-7 cancer cell lines and WRL68 normal cell lines. The concentration of Pd /TiO<sub>2</sub>NT that was required for 50% inhibition of MCF-7 and WRL68 cell inhibition was calculated. All data were expressed as means  $\pm$  standard deviations (SD). The statistical analysis was performed using Independent Samples Test (2-tailed(t-test )) at confidence levels of 95%.

From IC<sub>50</sub> values, listed in Table (2) it was found that the surface of titanium dioxide nanotubes modified by palladium nanoparticles has a higher toxicity than titanium nanotubes alone.

The toxicity of these nanomaterials Pd/TiO<sub>2</sub>NTs on cancer cells was observed to be twice as toxic when compared to normal cells.

Table 2 : Statistical data and IC<sub>50</sub> Values of Pd/TiO<sub>2</sub>NTs and TiO<sub>2</sub>NTs on cancer (MCF-7) cell lines and normal (WRL68) cell lines in time of exposure 48 hrs

Conc. $\mu\text{g/ml}$	Inhibition rate% (means $\pm$ standard deviation $\pm$ SD)			
	Pd/TiO <sub>2</sub> NT MCF-7	Pd/TiO <sub>2</sub> NT WRL68	TiO <sub>2</sub> NT MCF-7	TiO <sub>2</sub> NT WRL68
800	61.07 $\pm$ 0.848512	29.50 $\pm$ 0.560268	49.20 $\pm$ 0.136163	34.40 $\pm$ 0.577697
400	52.72 $\pm$ 0.377097	8.45 $\pm$ 0.625290	43.38 $\pm$ 0.0122317	12.89 $\pm$ 0.867106
200	42.38 $\pm$ 0.350487	7.65 $\pm$ 1.02573	30.97 $\pm$ 0.884123	8.84 $\pm$ 0.511783
100	34.89 $\pm$ 0.308837	6.34 $\pm$ 0.729618	20.94 $\pm$ 0.051394	7.30 $\pm$ 0.237557
50	20.44 $\pm$ 0.285001	6.15 $\pm$ 0.606028	15.80 $\pm$ 0.705143	5.98 $\pm$ 0.256689
25	10.87 $\pm$ 0.202429	5.90 $\pm$ 0.154448	10.50 $\pm$ 0.45254	4.30 $\pm$ 0.436534
12.5	9.99 $\pm$ 0.387874	3.23 $\pm$ 0.116762	7.03 $\pm$ 0.0417440	3.00 $\pm$ 0.325140
IC <sub>50</sub>	183	403	212	406

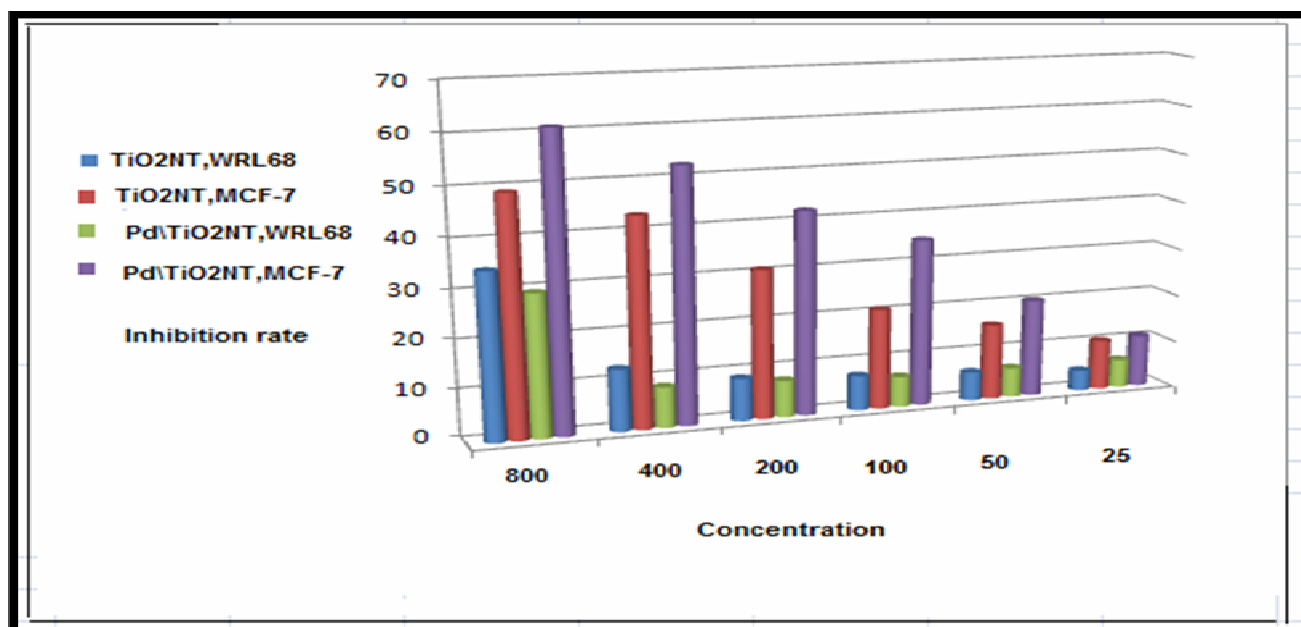


**Fig. 7 :** The percentage inhibition rate in MCF-7 cell line after treatment with TiO<sub>2</sub>NT, Pd/TiO<sub>2</sub>NT, 48 hrs compared to normal WRL68 cell lines

### Conclusion

Pd NPs were electrochemically deposited on titanium dioxide nanotubes support using palladium complexes as a source of palladium and prevent the nanoparticles aggregation. TEM analysis showed distorted spherical morphologies and tubes structures for the Pd nanoparticles and TiO<sub>2</sub>NTs respectively. Their elemental composition and chemical states were confirmed using EDX. The Pd/TiO<sub>2</sub>NTs shows a uniform and well dispersion of Pd NPs through the TiO<sub>2</sub>NTs with particle size less than 35 nm. The Pd/TiO<sub>2</sub>NTs has higher cytotoxic activity compared with TiO<sub>2</sub>NTs when using MCF-7 cancer cell lines.

**Funding :** This study does not receive any specific grant from funding agencies in the public, commercial or not for profit sectors.

### Compliance with ethical standards

**Conflict of interest:** The authors declare that they have no conflict of interest

### References

- Alias, M. and Bakir, Sh.R. (2017). Synthesis, Physico-Chemical characterization and cytotoxicity assay of Mannich base derivatives with heavy metal ions on RAW264.7 cell line", *Journal of Global Pharma Technology*, 9: 302-313.
- Alias, M. and Bakir, Sh.R. (2018). Synthesis, spectroscopic characterization and in vitro cytotoxicity assay of morpholine Mannich base derivatives of benzimidazole with some heavy metals", *Al-Nahrain Journal Sciences*.
- Al-Taweel, S.S. and Saud, S.R. (2016) New route for synthesis of pure anatase TiO<sub>2</sub> nanoparticles via ultrasound assisted sol-gel method, *Journal of Chemical and Pharmaceutical Research*, 2: 620-626.
- Ayal, A.K. (2017). Electrochemical synthesis and properties of cadmium selenide sensitised titania nanotubes for photoelectrochemical cells, Ph.D. dissertation, University Putra, Malaysia.
- Ayal, A.K.; Zainal, Z.; Lim, H.N.; Talib, Z.A.; Lim, Y-C.; Chang, S-K.; Samsudin, N.A.; Holi, A.M. and Amin, W.A.M. (2016). Electrochemical deposition of CdSe-sensitized TiO<sub>2</sub> nanotube arrays with enhanced photoelectrochemical performance for solar cell application, *Journal of Material Science: Materials in Electron* 27: 5204-5210.
- Boxi, S.S.; Mukherjee, K. and Paria, S. (2016). Ag-doped hollow TiO<sub>2</sub> nanoparticles as an effective green fungicide against *Fusarium solani* and *Venturia inaequalis* phytopathogens, *Nanotechnology*, 28: 085-103.
- Escada, A.L.; Nakazato, R.Z. and Claro, A.P.R.A. (2017) Influence of anodization parameters in the TiO<sub>2</sub> nanotubes formation on Ti-7.5 Mo alloy surface for biomedical application, *Materials Research*, 5:1282-1290.
- Feng, N.; Wang, Q.; Zheng, A.; Zhang, Z.; Fan, J.; Liu, S.B. and Deng, F. (2013). Understanding the high photocatalytic activity of (B, Ag)-codoped TiO<sub>2</sub> under solar-light irradiation with XPS, solid-state NMR, and DFT calculations. *Journal of the American Chemical Society*, 4: 1607-1616.
- Freshney, R.I. (2015). Culture of animal cells: a manual of basic technique and specialized applications. John Wiley & Sons.
- Indira, K.; Mudali, U.K.; Nishimura, T. and Rajendran, N. (2015). A review on TiO<sub>2</sub> nanotubes: influence of anodization parameters, formation mechanism, properties, corrosion behavior, and biomedical applications, *Journal of Bio-and Tribo-Corrosion*, 28.
- Jiang, Z.; Wei, W.; Mao, D.; Chen, C.; Shi, Y.; Lv, X. and Xie, J. (2015). Silver-loaded nitrogen-doped yolk-shell mesoporous TiO<sub>2</sub> hollow microspheres with enhanced visible light photocatalytic activity. *Nanoscale*, 2:784-797.
- Kittisakmontree, P.; Pongthawornsakun, B.; Yoshida, H.; Fujita, S.I.; Arai, M. and Panpranot, J. (2013). The liquid-phase hydrogenation of 1-heptyne over Pd-Au/TiO<sub>2</sub> catalysts prepared by the combination of

- incipient wetness impregnation and deposition-precipitation. *Journal of catalysis*, 297: 155-164.
- Leso, V. and IavicoliInt, I. (2018) Palladium Nanoparticles: Toxicological Effects and Potential Implications for Occupational Risk Assessment" *Journal Molecular Sciences*. 2018, 19:503-512.
- Lin, Y.; Qiqiang, W.; Xiaoming, Z.; Zhouping, W.; Wenshui, X. and Yuming, D. (2011). Synthesis of Ag/TiO<sub>2</sub> Core/Shell Nanoparticles with Antibacterial Properties. *Bulletin of the Korean Chemical Society*, 8: 2607-2610.
- Paul, K.K.; Ghosh, R. and Giri, P.K. (2016). Mechanism of strong visible light photocatalysis by Ag<sub>2</sub>O-nanoparticle-decorated monoclinic TiO<sub>2</sub>(B) porous nanorods, *Nanotechnology*, 27: 315-703.
- Robin, A.; de Almeida Ribeiro, M.B.; Rosa, J.L.; Nakazato, R.Z. and Silva, M.B. (2014). Formation of TiO<sub>2</sub> nanotube layer by anodization of titanium in ethylene glycol-H<sub>2</sub>O electrolyte. *Journal of Surface Engineered Materials and Advanced Technology* 3: 123-133.
- Saldan, I.; Semenyuk, Y.; Iryna, M. and Reshetnyak, O. (2015) Chemical synthesis and application of palladium nanoparticles., *Journal of Material Science*, 6: 2337-2354.
- Sara, M. and Sahar, S.M. (2012). Enhanced electrocatalytic activity of TiO<sub>2</sub>nanotubes modified with Pt and Pd nanoparticles: electro-oxidation of dopamine, uric acid and ascorbic acid", *International Journal of Theoretical and Applied Nanotechnology* 1: 73-78.
- Siddiqi, K.S. and Husen, A. (2016) Green Synthesis, Characterization and Uses of palladium /Platinum Nanoparticles, *Nanoscale Research. Letters*, 1: 482-491,
- Taziwa, R.; Meyer, E. and Takata, N. (2017) Structural and Raman Spectroscopic Characterization of C-TiO<sub>2</sub> Nanotubes Synthesized by a Template-Assisted Sol-Gel Technique, *Journal of nanoscience and nanotechnology Research*, 1: 1-11.
- Tsai, W.B.; Kao, J.Y.; Wu, T.M. and Cheng, W.T. (2016). Dispersion of Titanium Oxide Nanoparticles in Aqueous Solution with Anionic Stabilizer via Ultrasonic Wave. *Journal of Nanoparticles*, 2016: 1-9.
- Veena, V. (2018). TiO<sub>2</sub> and Pt/Pd Doped TiO<sub>2</sub> Up conversion Nanoparticles For Photodynamic Biomedical Applications. *IOSR Journal of Pharmacy and Biological Sciences (IOSR-JPBS)*,5: 01-10.